

Hypertension

JOURNAL OF THE AMERICAN HEART ASSOCIATION



Early and Late Systolic Wall Stress Differentially Relate to Myocardial Contraction and Relaxation in Middle-Aged Adults : The Asklepios Study

Julio A. Chirinos, Patrick Segers, Ernst R. Rietzschel, Marc L. De Buyzere, Muhammad W. Raja, Tom Claessens, Dirk De Bacquer, Martin St. John Sutton and Thierry C. Gillebert
on behalf of the Asklepios Investigators

Hypertension. 2013;61:296-303; originally published online January 2, 2013;

doi: 10.1161/HYPERTENSIONAHA.111.00530

Hypertension is published by the American Heart Association, 7272 Greenville Avenue, Dallas, TX 75231

Copyright © 2013 American Heart Association, Inc. All rights reserved.

Print ISSN: 0194-911X. Online ISSN: 1524-4563

The online version of this article, along with updated information and services, is located on the World Wide Web at:

<http://hyper.ahajournals.org/content/61/2/296>

Data Supplement (unedited) at:

<http://hyper.ahajournals.org/content/suppl/2012/12/31/HYPERTENSIONAHA.111.00530.DC1.html>

Permissions: Requests for permissions to reproduce figures, tables, or portions of articles originally published in *Hypertension* can be obtained via RightsLink, a service of the Copyright Clearance Center, not the Editorial Office. Once the online version of the published article for which permission is being requested is located, click Request Permissions in the middle column of the Web page under Services. Further information about this process is available in the [Permissions and Rights Question and Answer](#) document.

Reprints: Information about reprints can be found online at:

<http://www.lww.com/reprints>

Subscriptions: Information about subscribing to *Hypertension* is online at:

<http://hyper.ahajournals.org/subscriptions/>

Early and Late Systolic Wall Stress Differentially Relate to Myocardial Contraction and Relaxation in Middle-Aged Adults

The Asklepios Study

Julio A. Chirinos, Patrick Segers, Ernst R. Rietzschel,
Marc L. De Buyzere, Muhammad W. Raja, Tom Claessens, Dirk De Bacquer,
Martin St. John Sutton, Thierry C. Gillebert, on behalf of the Asklepios Investigators

Abstract—Experimental studies implicate late systolic load as a determinant of impaired left-ventricular relaxation. We aimed to assess the relationship between the myocardial loading sequence and left-ventricular contraction and relaxation. Time-resolved central pressure and time-resolved left-ventricular geometry were measured with carotid tonometry and speckle-tracking echocardiography, respectively, for computation of time-resolved ejection-phase myocardial wall stress (EP-MWS) among 1214 middle-aged adults without manifest cardiovascular disease from the general population. Early diastolic annular velocity and systolic annular velocities were measured with tissue Doppler imaging, and segment-averaged longitudinal strain was measured with speckle-tracking echocardiography. After adjustment for age, sex, and potential confounders, late EP-MWS was negatively associated with early diastolic mitral annular velocity (standardized $\beta=-0.25$; $P<0.0001$) and mitral inflow propagation velocity (standardized $\beta=-0.13$; $P=0.02$). In contrast, early EP-MWS was positively associated with early diastolic mitral annular velocity (standardized $\beta=0.18$; $P<0.0001$) and mitral inflow propagation velocity (standardized $\beta=0.22$; $P<0.0001$). A higher late EP-MWS predicted a lower systolic mitral annular velocity (standardized $\beta=-0.31$; $P<0.0001$) and lesser myocardial longitudinal strain (standardized $\beta=0.32$; $P<0.0001$), whereas a higher early EP-MWS was associated with a higher systolic mitral annular velocity (standardized $\beta=0.16$; $P=0.002$) and greater longitudinal strain (standardized $\beta=-0.24$; $P=0.002$). The loading sequence remained independently associated with early diastolic mitral annular velocity after adjustment for systolic mitral annular velocity or systolic longitudinal strain. In the context of available experimental data, our findings support the role of the myocardial loading sequence as a determinant of left-ventricular systolic and diastolic function. A loading sequence characterized by prominent late systolic wall stress was associated with lower longitudinal systolic function and diastolic relaxation. (*Hypertension*. 2013;61:296-303.) • [Online Data Supplement](#)

Key Words: afterload ■ diastolic function ■ loading sequence ■ myocardial function ■ myocardial wall stress ■ systolic function ■ tissue Doppler imaging

Afterload is recognized as an important determinant of myocardial function. Experimental animal studies demonstrate that increased afterload impacts diastolic relaxation.¹⁻⁵ Furthermore, studies in healthy instrumented dogs showed that, within physiological ranges, increased afterload results in differential responses in relaxation depending on its timing. In anesthetized open-chest dogs, mild-to-moderate increases in early systolic load resulted in unchanged or slightly enhanced relaxation, whereas increases in late systolic load resulted in a slow rate of diastolic ventricular pressure fall.^{2,6} This, however, was not observed in conscious dogs subjected to a similar protocol.⁷ More recently, greater late systolic pressure assessed

from a carotid pressure waveform⁸ or an invasively measured aortic pressure waveform⁹ has been shown to be associated with impaired early diastolic relaxation in humans. These studies implicate the loading sequence as a potential mechanistic determinant of diastolic relaxation.

Whereas analyses of central arterial pressure and pressure-flow relations are highly informative regarding arterial properties and ventricular-arterial interactions, they do not describe the time-varying mechanical load (stress) on the myocardium, which is determined by complex interactions between myocardial contractile elements, instantaneous left-ventricular (LV) geometry and the time-varying hydraulic

Received November 2, 2012; first decision December 1, 2012; revision accepted December 3, 2012.

From the Philadelphia VA Medical Center and University of Pennsylvania, Philadelphia, PA (J.A.C., M.W.R., M.S.J.S.); Institute Biomedical Technology (P.S., T.C.) and Department of Public Health (E.R.R., D.D.B.), Ghent University, Ghent, Belgium; Department of Cardiovascular Diseases, Ghent University Hospital, Ghent, Belgium (E.R.R., M.L.D.B., T.C.G.); and Department of Mechanics, University College Ghent, Ghent, Belgium (T.C.).

The online-only Data Supplement is available with this article at <http://hyper.ahajournals.org/lookup/suppl/doi:10.1161/HYPERTENSIONAHA.111.00530/-/DC1>.

Correspondence to Julio A. Chirinos, 3800 Woodland Ave (Rm-8B111), Philadelphia, PA 19104. E-mail Julio.chirinos@uphs.upenn.edu

© 2012 American Heart Association, Inc.

Hypertension is available at <http://hyper.ahajournals.org>

DOI:10.1161/HYPERTENSIONAHA.111.00530

load imposed by the arterial tree.¹⁰ All key determinants of myocardial stress (wall thickness, cavity size, and ventricular pressure, which in turn depends on arterial properties for any given flow delivered to the input impedance of the systemic circulation) exhibit marked variations during systole. Therefore, although aortic (and LV) pressure during systole is related to developed wall stress, LV geometric changes that occur during systole determine a profound but highly variable change in the relationship between LV pressure and wall stress.¹⁰ Consequently, time-varying myocardial stress estimations need to account for both time-varying pressure and time-varying geometry and are poorly represented by any single time-point measurement. The relationship between time-varying myocardial afterload and diastolic relaxation has not been previously investigated.

In this study, we tested the hypothesis that the timing of myocardial afterload (ie, early versus late systolic LV myocardial stress) is differentially associated with LV contraction and relaxation humans.

Methods

Study Population

We studied adults enrolled in the Asklepios study, a population-based sample of community-dwelling adults free of clinically apparent cardiovascular disease, aged 35 to 55 years from 2 Belgian communities.¹¹ This study was approved by the ethical committee of Ghent University Hospital and the University of Pennsylvania Institutional Review Board.

Central Pressure and Echocardiographic Measurements

Carotid artery applanation tonometry was performed using a Millar pen-type high-fidelity tonometer (SPT-301; Millar Instruments, Houston, TX).¹¹ Echocardiographic examinations were performed using a GE Vivid-7 ultrasound platform. Early diastolic (e') and systolic (S') septal mitral annular velocities were measured using pulsed-wave tissue Doppler from the apical 4-chamber view and were normalized for LV length.¹² Early diastolic LV inflow propagation velocity (V_{pe}) was measured with color M-mode as the slope of the isovelocity line from the mitral leaflet tips to a position 4 cm distal into the LV, using the first aliasing velocity.

Although e' was our primary noninvasive measure of diastolic relaxation, we performed sensitivity analyses using V_{pe} . We also assessed the effect of afterload on S' , which is influenced by the time-varying interaction between LV contractility and afterload during systole. Recently, S' was shown to be influenced by myocardial contractility (even in the presence of a normal ejection fraction), longitudinal fiber shortening, and torsional deformation,¹³ and to be an independent predictor of mortality in a general population sample with normal LV ejection fraction.¹⁴ In addition to S' , we also assessed average longitudinal strain using speckle-tracking echocardiography as described below.

LV end-diastolic volume and LV mass were calculated with the area-length method. LV sphericity index was obtained by dividing the width of the LV measured at the basal aspect of the papillary muscles by LV length, expressed as a percentage as previously described.

Assessment of Time-Resolved Myocardial Wall Stress

Speckle tracking was performed using an echoPAC workstation (GE Healthcare; Waukesha, WI) as previously described.¹⁰ Briefly, a region of interest was prescribed in the parasternal short-axis view at the level of the chordae tendineae to obtain an exact fit with LV wall thickness, and the software was used to automatically track the wall at every time point in the cardiac cycle. Speckle tracking was also

performed from the apical 4-chamber view to assess instantaneous LV length in an interrogation angle-independent manner. Only cases in which reliable tracking of endocardial and epicardial borders was visually ascertained in both long and short-axis views and in which ≤ 1 segment was labeled by the automated software as being tracked unreliably were processed further. Time-resolved numeric values derived from speckle tracking were exported from the echoPAC software for further processing in custom-designed software written in Matlab (The Mathworks, Natick, MA). We computed time-resolved short-axis cross-sectional area and LV length as previously described in detail,¹⁰ allowing for assessments of time-resolved area-length volume measurements. The carotid pressure curve was time-aligned with geometric data using LV outflow velocity information (Figure 1A–1E), assessed with pulsed-wave Doppler interrogation of the outflow tract, to account for the brief delay between aortic and carotid pressure phenomena, as previously described.¹⁰ Time-resolved myocardial wall stress was computed according to Arts¹⁵:

$$\text{Myocardial Wall ("Fiber") Stress} = P/[1/3 \ln(1 + V_w/V_{LV})]$$

where P =pressure, \ln =natural logarithm, V_w =wall volume, and V_{LV} =ventricular cavity volume (computed at each time point with the area-length method). This method does not neglect radially directed forces or forces generated within the wall that oppose fiber shortening, which vary significantly with cavity and wall thickness and can interfere with direct comparisons of myocardial stress at different times during ejection.

Representative time-resolved short-axis LV wall thickness and cavity area obtained from the parasternal short-axis view are shown in Figure 1A and 1B. Figure 1C and 1D shows representative time-resolved changes in LV cavity size and changes in LV cavity length resulting from displacement of the base toward the apex and from apical cap thickening. Figure 2A and 2B shows a central pressure waveform and ejection-phase myocardial stress, respectively. To assess the myocardial loading sequence, we separately computed the myocardial stress-time integral (area under the curve) in the first half of ejection (early ejection-phase stress-time integral) and the second half of ejection (late ejection-phase stress-time integral). For simplicity, throughout the remainder of the article we refer to these time integrals as early ejection-phase wall stress and late ejection-phase wall stress, respectively. In repeated (sequential) measurements in 8 individuals, the coefficients of variation for early ejection-phase wall stress, late ejection-phase wall stress, and the ratio of late/early systolic stress were 7.94%, 8.22%, and 5.24%, respectively.

Speckle-tracking echocardiography data were also used to compute systolic longitudinal Langrangian strain, averaged from interrogated segments in the 4-chamber view, defined as the change of myocardial fiber length during stress in systole (L_1) compared with its original length (L_0) in a relaxed state at end-diastole¹⁶: $(L_1 - L_0)/L_0$.

Statistical Analysis

The relationship between early and late systolic wall stress and indices of myocardial function was analyzed using linear regression. Multivariate models were adjusted for total cholesterol, high-density lipoprotein-cholesterol, triglycerides, estimated glomerular filtration rate, serum C-reactive protein, current smoking, diabetes mellitus, menopausal status, antihypertensive medication use, and heart rate. Although the formula we used for computation of LV myocardial stress is valid for axisymmetric ventricular geometry regardless of sphericity,¹⁵ we also adjusted for LV sphericity to better account for geometric factors that may impact diastolic relaxation longitudinal velocities and relaxation independently of wall stress. All P values are 2-tailed. Statistical significance was defined as $\alpha < 0.05$. Statistical analyses were performed using SPSS for Windows v17 (SPSS Inc, Chicago, IL).

Results

Table 1 compares subjects enrolled in the Asklepios cohort with and without available time-resolved myocardial stress (ie, included versus not included in this study). Males represented

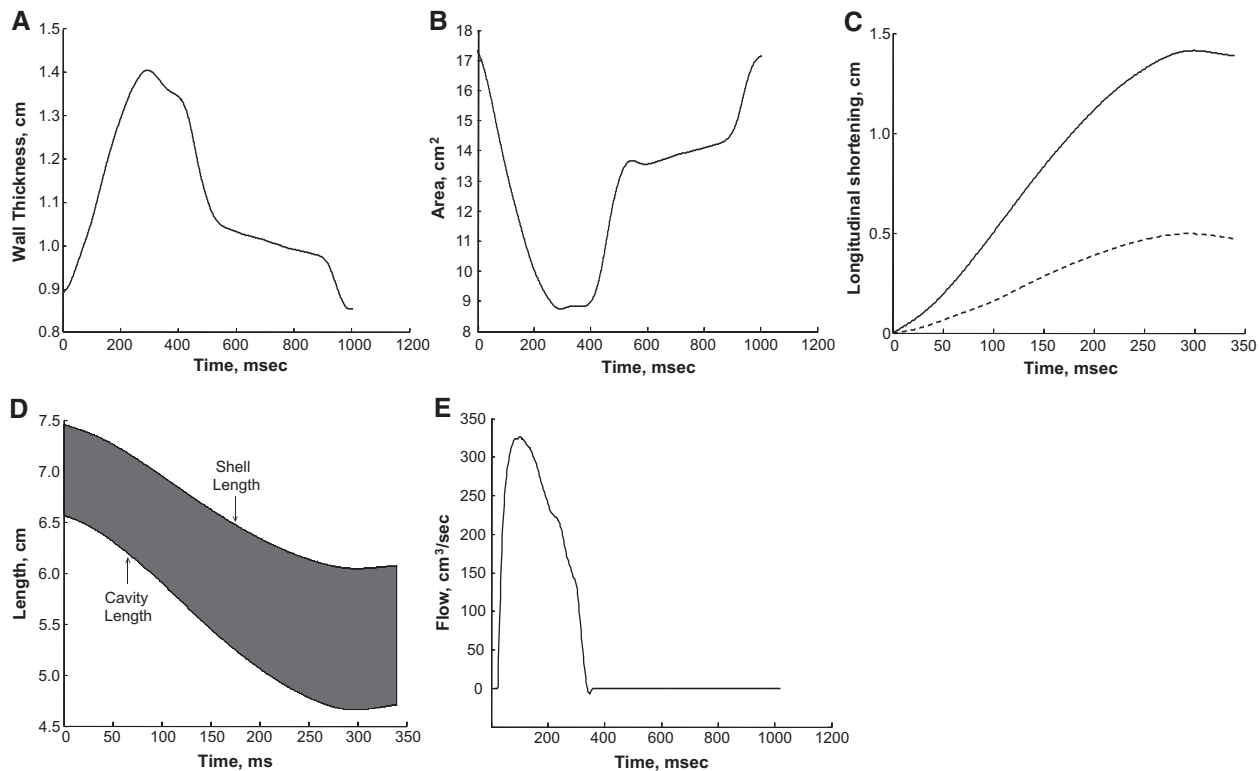


Figure 1. Assessment of time-resolved ventricular geometry with speckle-tracking echocardiography. **A**, Average wall thickness from a parasternal short-axis view at the base of the left ventricle (LV). **B**, Time-resolved cavity area from the same view. **C**, Longitudinal shortening of the LV cavity during ejection. This represents the reduction in LV length that occurs from mitral annular descent toward the apex during ejection. The dotted line represents the additional reduction in LV cavity length from apical cap thickening. With these data, time-resolved LV length of the cavity and the epicardial shell during ejection are computed, as shown in **D**. **E**, The blood outflow that occurs as a direct result of LV geometric changes and can be used to time-align cardiac geometry with central pressure events recorded at the carotid artery.

a higher proportion of subjects included in this study. There were minimal but statistically significant differences in age, body size, and various other measured parameters between subjects included in this study versus those not included in this substudy.

Relationship Between the Loading Sequence and Early Diastolic Relaxation

Table 2 shows a multivariate model in which early and late ejection-phase wall stress are assessed as independent predictors of e' . Late ejection-phase wall stress was negatively associated with e' (standardized $\beta = -0.25$; $P < 0.0001$). In contrast,

early ejection-phase wall stress was positively associated with e' (standardized $\beta = 0.18$; $P < 0.0001$). Increasing age (standardized $\beta = -0.34$; $P < 0.0001$) and body weight (standardized $\beta = -0.38$; $P < 0.0001$) were also associated with lower e' . Other predictors of e' included sex, total cholesterol, high-density lipoprotein-cholesterol, and LV sphericity, although the adjusted association between these measures was weaker than that seen for age, body weight, and wall stress. This model predicted 46% of the interindividual variability in e' .

Table S1 in the online-only Data Supplement shows an analogous model in which the predicted variable is V_{pe} , rather than e' . Early ejection-phase wall stress was the

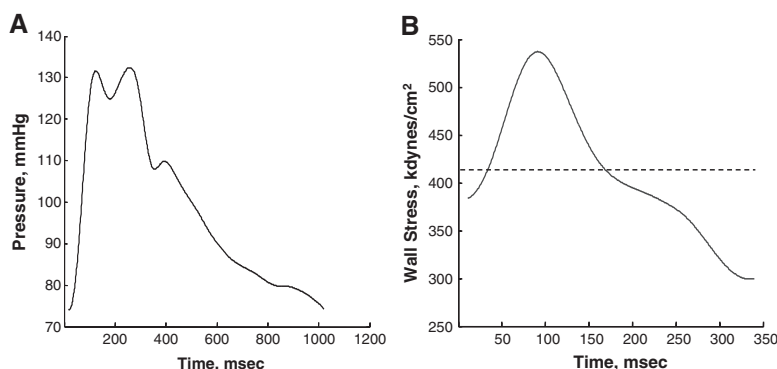


Figure 2. Computation of time-resolved ejection-phase wall stress from geometric data and central pressures. **A**, A central pressure waveform, which is determined by the inflow of blood into the arterial system and the mechanical arterial properties of the arterial tree. **B**, A time-resolved ejection-phase stress curve, computed from time-resolved pressure and time-resolved left-ventricular (LV) geometric measurements; the dotted line shows mean ejection-phase stress. Note that the time-axis in **B** corresponds only to the ejection phase, whereas the pressure waveform corresponds to an entire cardiac cycle. Early ejection-phase wall stress was quantified as the stress-time integral (area under the curve) during the first half of ejection, whereas late ejection-phase myocardial wall stress was quantified as the stress-time integral during the second half of ejection.

Table 1. General Characteristics of Asklepios Study Subjects Included and Not Included in This Substudy

Variable	Included in This Substudy (n=1214)	Not Included in This Substudy (n=1310)
Age, y*	45.1 (40.5, 50.2)	46.5 (41.5, 51.5)
Male sex, %*	54.6	42.8
Body height, m*	170 (164, 177)	168 (162, 175)
Body weight, kg†	72 (62.8, 82.4)	74.1 (63.1, 84.7)
Body mass index, kg/m ² *	24.8 (22.7, 27.2)	25.6 (23, 29.2)
Hypertension, %	27	30.5
Diabetes mellitus, %	1.2	2.0
LDL-cholesterol, mg/dL	127 (107, 152)	127 (107, 152)
HDL-cholesterol, mg/dL	61 (51, 74)	62 (51, 75)
Triglycerides, mg/dL†	88 (64, 127)	93 (67, 134)
Current smoking, %	21.6	20.1
C-reactive protein (mg/L)*	1.10 (0.51, 2.13)	1.40 (0.67, 6312)
Left-ventricular mass, g	143 (115, 176)	140 (111, 176)
Left-ventricular mass index, g/ height in m ^{1.7}	58 (49, 69)	58 (48, 70)
Left-ventricular end-diastolic volume index, mL/ BSA in m ² *	57 (49, 67)	53 (46, 63)
Left-ventricular ejection fraction, %	66 (60, 71)	67 (62, 72)
Systolic mitral annular velocity, cm/s	7.8 (7.1, 8.5)	7.8 (7.1, 8.6)
Early diastolic mitral annular velocity, cm/s	9.1 (7.8, 11)	8.9 (7.5, 10)
LV inflow propagation velocity, cm/s*	71 (60, 85)	74 (63, 90)
NT-proBNP (pg/mL)*	39 (20, 72)	46 (25, 81)
Sphericity index, %	57 (52, 61)	57 (52, 61)
Heart rate, bpm	65 (58, 71)	66 (59, 73)
Longitudinal strain, %	-18.2 (-19.8, -16.4)	
Early ejection-phase MWS (kdynes-cm ⁻² -s)	79.6 (70.9, 90.8)	----
Late ejection-phase MWS (kdynes-cm ⁻² -s)	65.1 (56.8, 75.5)	----
Late/early ejection-phase MWS	0.82 (0.76, 0.88)	----

Values indicate median (interquartile range) or percentage. BSA indicates body surface area; HDL, high-density lipoprotein; LDL, low-density lipoprotein; LV, left ventricular; MWS, myocardial wall stress; and NT-proBNP, N-terminal pro-brain natriuretic peptide.

* $P<0.0001$.

† $P<0.05$.

single most important independent predictor of (higher) Vpe (standardized $\beta=0.22$; $P<0.0001$), whereas late ejection-phase wall stress was negatively associated with Vpe (standardized $\beta=-0.13$; $P=0.017$). Age (standardized $\beta=-0.19$; $P<0.0001$), LV sphericity (standardized $\beta=-0.14$; $P<0.0001$), and high-density lipoprotein-cholesterol (standardized $\beta=0.10$; $P=0.004$) were also independently associated with Vpe.

Relationship Between Early/Late Systolic Wall Stress and Longitudinal Systolic Shortening Indices

Table 3 shows a multivariate model in which early and late ejection-phase wall stress are assessed as independent predictors of S'. In this model, late ejection-phase wall stress was the single most important predictor of (lower) S' (standardized $\beta=-0.31$; $P<0.0001$), whereas a higher early ejection-phase wall stress was associated with a high S' velocity (standardized $\beta=0.16$; $P=0.002$). Greater body weight (standardized $\beta=-0.24$; $P<0.0001$), increasing age (standardized $\beta=-0.07$; $P<0.018$), and male sex (standardized $\beta=-0.19$; $P<0.0001$) were also associated with lower S', whereas LV sphericity

(standardized $\beta=0.11$; $P=0.0001$) and heart rate (standardized $\beta=0.23$; $P<0.0001$) were positively associated with S'. This model explained 23% of the interindividual variability in S'.

An analogous model in which the independent variable is systolic longitudinal strain is shown in Table 4. Note that lower (more negative) values of longitudinal strain indicate greater deformation and, therefore, positive coefficients indicate an inverse relationship with shortening, whereas negative coefficients indicate a direct one. In this model, late ejection-phase wall stress was the single most important predictor of lower longitudinal shortening (standardized $\beta=0.32$; $P<0.0001$), whereas a higher early ejection-phase wall stress was associated with a greater longitudinal shortening (standardized $\beta=-0.24$; $P<0.0001$). Other predictors of longitudinal strain included male sex (standardized $\beta=0.19$; $P<0.0001$), high-density lipoprotein-cholesterol (standardized $\beta=-0.09$; $P=0.006$), LV sphericity (standardized $\beta=-0.18$; $P<0.0001$), and heart rate (standardized $\beta=0.16$; $P<0.0001$). This model explained 18% of the interindividual variability in peak systolic longitudinal strain.

Table 2. Early and Late Systolic Stress as Predictors of Early Diastolic Mitral Annular Velocity in a Multivariate Model ($R^2=0.46$)

Independent Variables	Standardized Coefficient β	P Value
(Constant)		<0.0001
Late ejection-phase MWS, $\text{kdynes}\cdot\text{cm}^{-2}\cdot\text{s}$	-0.25	<0.0001
Early ejection-phase MWS, $\text{kdynes}\cdot\text{cm}^{-2}\cdot\text{s}$	0.18	<0.0001
Age, y	-0.34	<0.0001
Male sex	-0.17	<0.0001
Body height, m	0.068	0.06
Body weight, kg	-0.38	<0.0001
Total cholesterol, mg/dL	-0.067	0.005
HDL-cholesterol, mg/dL	0.073	0.008
Triglycerides, mg/dL	-0.027	0.27
Estimated GFR, $\text{mL}\cdot\text{min}^{-1}\cdot 1.73\text{ m}^{-2}$	-0.008	0.71
High-sensitive CRP (ln-transformed), mg/dL	-0.002	0.91
Current smoking	0.025	0.26
Diabetes mellitus	0.005	0.84
LV sphericity	0.14	<0.0001
Antihypertensive medication use	-0.027	0.23
Heart rate, bpm	-0.017	0.47

CRP indicates C-reactive protein; GFR, glomerular filtration rate; HDL, high-density lipoprotein; LV, left ventricular; and MWS, myocardial wall stress.

Relationship Between Wall Stress and Diastolic Relaxation After Adjustment for Longitudinal Systolic Shortening

After adjustment for S' and all covariates shown in Table 2, early systolic wall stress remained independently positively associated with e' (standardized $\beta=0.13$; $P=0.002$), whereas late systolic wall stress was independently negatively associated with e' (standardized $\beta=-0.15$; $P<0.0001$). Late systolic wall stress also remained significantly associated with e' after adjustment for longitudinal strain (standardized $\beta=-0.14$; $P=0.003$), end-systolic volume (standardized $\beta=-0.23$; $P<0.0001$), LV ejection fraction (standardized $\beta=-0.21$; $P<0.0001$), or LV mass (standardized $\beta=-0.19$; $P<0.0001$).

Discussion

In this study, we assessed the relationship between myocardial contraction, relaxation, and time-resolved ejection-phase myocardial wall stress, assessed noninvasively in a large population-based sample of middle-aged adults without manifest cardiovascular disease. We report, for the first time, that early ejection-phase wall stress is positively associated, whereas late systolic ejection-phase wall stress is negatively associated with noninvasive estimates of diastolic relaxation (e' and V_{pe}). Similar associations were observed for noninvasive estimates of systolic function (peak S' and peak systolic longitudinal strain). However, the observed relationships between the loading sequence and e' and V_{pe} persisted after adjustment for S' or peak systolic longitudinal strain. Our findings, therefore, indicate an independent association

Table 3. Early and Late Systolic Stress as Predictors of Peak Systolic Mitral Annular Velocity in a Multivariate Model ($R^2=0.23$)

Independent Variables	Standardized Coefficient β	P Value
(Constant)		
Late ejection-phase MWS, $\text{kdynes}\cdot\text{cm}^{-2}\cdot\text{s}$	-0.31	<0.0001
Early ejection-phase MWS, $\text{kdynes}\cdot\text{cm}^{-2}\cdot\text{s}$	0.16	0.002
Age, y	-0.066	0.018
Male sex	-0.19	<0.0001
Body height, m	0.077	0.07
Body weight, kg	-0.24	<0.0001
Total cholesterol, mg/dL	-0.035	0.21
HDL-cholesterol, mg/dL	0.001	0.98
Triglycerides, mg/dL	0.018	0.54
Estimated GFR, $\text{mL}\cdot\text{min}^{-1}\cdot 1.73\text{ m}^{-2}$	-0.016	0.55
High-sensitive CRP (ln-transformed), mg/dL	0.043	0.11
Current smoking	-0.039	0.15
Diabetes mellitus	-0.003	0.90
LV sphericity, %	0.11	0.0001
Antihypertensive medication use	0.005	0.84
Heart rate, bpm	0.23	<0.0001

CRP indicates C-reactive protein; GFR, glomerular filtration rate; HDL, high-density lipoprotein; LV, left ventricular; and MWS, myocardial wall stress.

between the myocardial loading sequence and LV systolic and diastolic function.

Diastolic LV relaxation is an important process that promotes LV filling during the early diastole, allowing for cardiac output adaptations to changes in loading conditions, inotropic stimulation, and heart rate. Most earlier experimental studies associated (markedly) increased afterload with slower relaxation,^{4,5} but some studies showed that, with mild-to-moderate increases of afterload, relaxation was accelerated,⁶ a behavior consistent with isolated cardiac muscle findings.¹⁷ A recent study showed that, among patients with normal LV systolic function undergoing coronary artery bypass surgery, peak systolic LV pressure >230 mm Hg can develop in response to aortic clamping (an intervention that increases early systolic load), without slowing of relaxation and no increase in filling pressures, hence no diastolic dysfunction.¹⁸ The effect of late systolic load on LV relaxation has also been the subject of previous studies. Brutsaert et al¹⁹ initiated the concept of load-dependence of relaxation and described acceleration of relaxation and early termination of a twitch contraction in response to late systolic load clamps. This, however, was only observed in isolated cardiac muscle with isotonic-isometric relaxation sequence and isometrically contracting hearts subjected to volume clamps.²⁰ Acceleration of relaxation was induced at most to a limited extent in the intact ejecting ventricle,^{6,7} but the clinical relevance of this finding is questionable. In more physiological working conditions, both muscle²¹ and the intact ejecting ventricle² predominantly responded to late systolic load with delayed

Table 4. Early and Late Systolic Stress as Predictors of Peak Systolic Longitudinal Strain in a Multivariate Model ($R^2=0.18$)

Independent Variables	Standardized Coefficient β	P Value
(Constant)		<0.0001
Late ejection-phase MWS, $\text{kdynes}\cdot\text{cm}^{-2}\cdot\text{s}$	0.32	<0.0001
Early ejection-phase MWS, $\text{kdynes}\cdot\text{cm}^{-2}\cdot\text{s}$	-0.24	<0.0001
Age, y	0.02	0.52
Male sex	0.19	<0.0001
Body height, m	0.05	0.25
Body weight, kg	0.02	0.65
Total cholesterol, mg/dL	0.05	0.11
HDL-cholesterol, mg/dL	-0.09	0.006
Triglycerides, mg/dL	0.04	0.25
Estimated GFR, $\text{mL}\cdot\text{min}^{-1}\cdot 1.73\text{ m}^{-2}$	-0.04	0.15
High-sensitive CRP (ln-transformed), mg/dL	0.03	0.30
Current smoking	-0.02	0.51
Diabetes mellitus	0.03	0.31
LV sphericity	-0.18	<0.0001
Antihypertensive medication use	0.02	0.46
Heart rate, bpm	0.16	<0.0001

CRP indicates C-reactive protein; GFR, glomerular filtration rate; HDL, high-density lipoprotein; LV, left ventricular; and MWS, myocardial wall stress.

relaxation, confirming the seminal finding of Hori.²² In line with these canine studies, Yano et al²³ studied humans during cardiac catheterization and reported that femoral artery compression induced a reflected wave that arrived to the aorta in late systole, which resulted in prolonged relaxation. The within-beat effects of systolic clamps on diastolic relaxation have been explained on the basis of the differential effect of early versus late load on the number of interacting cross-bridges.³ Loading during active cross-bridge formation (early systolic load) increases the number of interacting cross-bridges (cooperative activity),³ a physiological mechanism that allows adequate matching of the number of cross-bridges with systolic load. However, when increased load occurs after the onset of myocardial relaxation, the number of interacting cross-bridges can no longer adapt. Under these circumstances, a mismatch between the number of cross-bridges and load may occur, increasing the stress imposed on individual cross-bridges and decreasing cross-bridge cycling.³ It is important to note that the timing of transition from myocardial contraction to relaxation differs from the timing of transition from ventricular systole to diastole, normally occurs early during the ejection phase,^{3,24,25} and is related to the descending limb of the myocyte cytoplasmic calcium transient.^{3,24}

Whereas experimental load clamps and acute catheterization studies represent valuable approaches to isolate the effects of afterload on relaxation, they cannot be extrapolated to the physiology of free-living individuals, where more progressive load changes occur and multiple additional factors influence relaxation. Therefore, studies are needed to clarify

the naturally occurring relationship between the LV loading sequence and relaxation. Our study is novel because it is the first to assess the relationship between relaxation and time-resolved myocardial loading using not only central pressure but also LV geometric data, an important determinant of wall stress. Furthermore, we report, for the first time, not only that late systolic load is associated with slower relaxation, but that in models that adjust for late systolic load, early systolic load is associated with faster relaxation. Our large, population-based sampling strategy, carefully standardized assessments, use of sophisticated noninvasive methods for wall stress estimations, and use of independent measures of diastolic relaxation (e' and V_{pe} , which provided highly consistent results) and systolic longitudinal shortening (S' and peak systolic longitudinal strain) are strengths of our study.

We found that the loading sequence was also related to S' and longitudinal LV shortening. The positive relationship between early load and S' is somewhat counterintuitive. A possible explanation would be that contractility determines wall stress and not the other way around; therefore, subjects with greater contractility may develop a higher peak wall stress compared with those with lower contractility. Other possible underlying mechanisms may include neurohumoral adjustments associated with higher peak (or early) systolic wall stress and the induction of cooperative activity by myocardial loading during cross-bridge formation. It is interesting to note that, after adjustment for systolic LV long-axis shortening, the value of the coefficient for late stress as a predictor of e' decreased (by $\approx 45\%$), suggesting that the relationship between late systolic wall stress and systolic shortening partially underlies the relationship between late systolic wall stress and e' . These findings are best interpreted in light of recent data demonstrating that, in addition to early diastolic load (lengthening load), e' is determined not only by intrinsic myocardial relaxation, but also prominently influenced by restoring forces, particularly in the presence of normal LV function.²⁶ The amount of potential energy stored during contraction and released during relaxation is negatively related to end-systolic length and volume. The ability to reduce end-systolic length or volume, therefore, contributes to the active restoration of LV dimensions in early diastole and enhances the rate of relaxation.^{1,27} However, we believe that restoring forces are unlikely to fully explain the relationship between the loading sequence and e' , because this persisted after adjustment for LV end-systolic length, end-systolic volume, or S' . Further studies regarding the mechanisms that link the contraction history and myocardial relaxation at the molecular level are required.

The observation that late systolic wall stress relates to adverse parameters of myocardial and LV function in this population is consistent with animal, clinical, and epidemiological data, which strongly suggest that wave reflections are important determinants of LV dysfunction,^{28–30} as well as recent data from the Multiethnic Study of Atherosclerosis indicating that wave reflection magnitude strongly predicts the risk of incident heart failure in the general population.^{31,32} It is interesting to note that this relationship occurs despite the fact that wall stress in late systole is much lower than wall stress in early systole, as a result of the geometric changes associated with myocardial contraction and blood ejection. Jointly, these

findings further suggest that the loading sequence may be more important than absolute stress levels, per se. Although absolute wall stress is lower in late systole, the myocardium may be particularly vulnerable to even small wall stress increases during this period of time. This may be a result of intrinsic differences in cellular processes between early and late ejection. During early ejection, active development of fiber cross-bridges occurs in the myocardium, whereas a transition from contraction to relaxation occurs in mid- to-late systole, during which increases in load may be particularly deleterious, leading to more hypertrophy and abnormal diastolic relaxation.^{2,33} The differential effect of time-varying myocardial afterload on cellular processes taking place in early and late ejection is, therefore, an important area for future research.

Our findings should be interpreted in the context of the determinants of time-resolved myocardial wall stress, which include the various arterial properties determining the input impedance of the systemic arterial tree as well as the pattern of myocardial contraction leading to changes in LV geometry. Early versus late systolic myocardial wall stress demonstrates finite relationships with specific arterial properties. We have recently shown in this population that, whereas systemic vascular resistance is a strong determinant of both early and late wall stress, aortic characteristic impedance determines ejection-phase systolic wall stress, whereas wall stress at the end of systole is related to reflection magnitude.³⁴

Our study has limitations. Our observational study does not prove causality. Unmeasured mechanisms (such as neurohormonal factors or genetic polymorphisms) may lead to noncausal associations between time-resolved wall stress and relaxation. Mitral annular velocities assessed via tissue Doppler imaging are affected by the interrogation angle and do not distinguish between in-plane translation of the heart and shortening. We only interrogated septal mitral annular tissue velocities. It is a reasonable assumption that septal mitral annular motion is representative for global LV longitudinal systolic and diastolic function in a healthy population, where cardiac function is within the normal range and fairly homogeneous. In addition, our assessments of LV volumes using 2D-measurements rely on geometric assumptions and are, thus, approximations. We note, however, that methods were applied uniformly to all study participants. We limited our study to a population without manifest cardiovascular disease, to assess these physiological relationships before the appearance of clinically apparent myocardial dysfunction. Although the strength of relationships observed in this relatively healthy population were generally comparable with (and in some instances greater than) relationships observed for known important risk factors for heart failure in the general population, our cross-sectional study cannot yet assess whether these relationships are relevant to the prospective risk of clinically relevant myocardial dysfunction or heart failure.

Perspectives

Our findings indicate that in unselected middle-aged adults, greater early systolic wall stress is associated with greater longitudinal systolic function and enhanced early diastolic relaxation. In contrast, late systolic myocardial wall stress was independently associated with decreased early diastolic

relaxation and decreased longitudinal systolic function. Our findings support the role of time-varying myocardial afterload as a determinant of myocardial relaxation. Future mechanistic studies regarding the role of loading sequence on myocardial contraction-relaxation coupling may enhance our understanding of the pathophysiology of abnormal myocardial function and may aid in identifying potential targets or interventions to improve LV diastolic relaxation and systemic adaptations to increased afterload.

Sources of Funding

This study was supported by Fonds voor Wetenschappelijk Onderzoek Vlaanderen grant G.0.838.10 and Edna G. Kynett Memorial Foundation (Dr Chirinos).

Disclosures

Dr Chirinos has received significant (>\$10 000) grants from the National Institutes of Health and the American Heart Association for research studies related to arterial hemodynamics and has received minor support (equipment loans) from Atcor Medical, Cardiodynamics, and APC cardiovascular.

References

1. Zile MR, Gaasch WH. Mechanical loads and the isovolumic and filling indices of left ventricular relaxation. *Prog Cardiovasc Dis*. 1990;32:333–346.
2. Gillebert TC, Lew WY. Influence of systolic pressure profile on rate of left ventricular pressure fall. *Am J Physiol*. 1991;261(3 pt 2):H805–H813.
3. Gillebert TC, Leite-Moreira AF, De Hert SG. Load dependent diastolic dysfunction in heart failure. *Heart Fail Rev*. 2000;5:345–355.
4. Gaasch WH, Blaustein AS, Andrias CW, Donahue RP, Avitall B. Myocardial relaxation. II. Hemodynamic determinants of rate of left ventricular isovolumic pressure decline. *Am J Physiol*. 1980;239:H1–H6.
5. Karliner JS, LeWinter MM, Mahler F, Engler R, O'Rourke RA. Pharmacologic and hemodynamic influences on the rate of isovolumic left ventricular relaxation in the normal conscious dog. *J Clin Invest*. 1977;60:511–521.
6. Leite-Moreira AF, Gillebert TC. Nonuniform course of left ventricular pressure fall and its regulation by load and contractile state. *Circulation*. 1994;90:2481–2491.
7. Zile MR, Gaasch WH. Load-dependent left ventricular relaxation in conscious dogs. *Am J Physiol*. 1991;261(3 pt 2):H691–H699.
8. Borlaug BA, Melenovsky V, Redfield MM, Kessler K, Chang HJ, Abraham TP, Kass DA. Impact of arterial load and loading sequence on left ventricular tissue velocities in humans. *J Am Coll Cardiol*. 2007;50:1570–1577.
9. Fujimoto N, Onishi K, Tanabe M, Dohi K, Funabiki K, Kurita T, Yamanaka T, Nakajima K, Ito M, Nobori T, Nakano T. Nitroglycerin improves left ventricular relaxation by changing systolic loading sequence in patients with excessive arterial load. *J Cardiovasc Pharmacol*. 2005;45:211–216.
10. Chirinos JA, Segers P, Gupta AK, Swillens A, Rietzschel ER, De Buyzere ML, Kirkpatrick JN, Gillebert TC, Wang Y, Keane MG, Townsend R, Ferrari VA, Wiegiers SE, St John Sutton M. Time-varying myocardial stress and systolic pressure-stress relationship: role in myocardial-arterial coupling in hypertension. *Circulation*. 2009;119:2798–2807.
11. Segers P, Rietzschel ER, De Buyzere ML, Vermeersch SJ, De Bacquer D, Van Bortel LM, De Backer G, Gillebert TC, Verdonck PR; Asklepios investigators. Noninvasive (input) impedance, pulse wave velocity, and wave reflection in healthy middle-aged men and women. *Hypertension*. 2007;49:1248–1255.
12. Batterham A, Shave R, Oxborough D, Whyte G, George K. Longitudinal plane colour tissue-Doppler myocardial velocities and their association with left ventricular length, volume, and mass in humans. *Eur J Echocardiogr*. 2008;9:542–546.
13. Seo JS, Kim DH, Kim WJ, Song JM, Kang DH, Song JK. Peak systolic velocity of mitral annular longitudinal movement measured by pulsed tissue Doppler imaging as an index of global left ventricular contractility. *Am J Physiol Heart Circ Physiol*. 2010;298:H1608–H1615.
14. Mogelvang R, Sogaard P, Pedersen SA, Olsen NT, Marott JL, Schnohr P, Goetze JP, Jensen JS. Cardiac dysfunction assessed by echocardiographic tissue Doppler imaging is an independent predictor of mortality in the general population. *Circulation*. 2009;119:2679–2685.

15. Arts T, Bovendeerd PH, Prinzen FW, Reneman RS. Relation between left ventricular cavity pressure and volume and systolic fiber stress and strain in the wall. *Biophys J*. 1991;59:93–102.
16. Blessberger H, Binder T. NON-invasive imaging: two dimensional speckle tracking echocardiography: basic principles. *Heart*. 2010;96:716–722.
17. Wiegner AW, Bing SH. Isometric relaxation of rat myocardium at end-systolic fiber length. *Circ Res*. 1978;43:865–869.
18. Leite-Moreira AF, Lourenço AP, Roncon-Albuquerque R Jr, Henriques-Coelho T, Amorim MJ, Almeida J, Pinho P, Gillebert TC. Diastolic tolerance to systolic pressures closely reflects systolic performance in patients with coronary heart disease. *Basic Res Cardiol*. 2012;107:251.
19. Brutsaert DL, de Clerck NM, Goethals MA, Housmans PR. Relaxation of ventricular cardiac muscle. *J Physiol (Lond)*. 1978;283:469–480.
20. Ariel Y, Gaasch WH, Bogen DK, McMahon TA. Load-dependent relaxation with late systolic volume steps: servo-pump studies in the intact canine heart. *Circulation*. 1987;75:1287–1294.
21. Gillebert TC, Sys SU, Brutsaert DL. Influence of loading patterns on peak length-tension relation and on relaxation in cardiac muscle. *J Am Coll Cardiol*. 1989;13:483–490.
22. Hori M, Inoue M, Kitakaze M, Tsujioka K, Ishida Y, Fukunami M, Nakajima S, Kitabatake A, Abe H. Loading sequence is a major determinant of afterload-dependent relaxation in intact canine heart. *Am J Physiol*. 1985;249(4 pt 2):H747–H754.
23. Yano M, Kohno M, Kobayashi S, Obayashi M, Seki K, Ohkusa T, Miura T, Fujii T, Matsuzaki M. Influence of timing and magnitude of arterial wave reflection on left ventricular relaxation. *Am J Physiol Heart Circ Physiol*. 2001;280:H1846–H1852.
24. Solomon SB, Nikolic SD, Frater RW, Yellin EL. Contraction-relaxation coupling: determination of the onset of diastole. *Am J Physiol*. 1999;277(1 pt 2):H23–H27.
25. Chung CS, Kovács SJ. Pressure phase-plane based determination of the onset of left ventricular relaxation. *Cardiovasc Eng*. 2007;7:162–171.
26. Opdahl A, Remme EW, Helle-Valle T, Lyseggen E, Vartdal T, Pettersen E, Edvardsen T, Smiseth OA. Determinants of left ventricular early-diastolic lengthening velocity: independent contributions from left ventricular relaxation, restoring forces, and lengthening load. *Circulation*. 2009;119:2578–2586.
27. Courtois M, Mechem CJ, Barzilai B, Ludbrook PA. Factors related to end-systolic volume are important determinants of peak early diastolic transmitral flow velocity. *Circulation*. 1992;85:1132–1138.
28. Kobayashi S, Yano M, Kohno M, Obayashi M, Hisamatsu Y, Ryoike T, Ohkusa T, Yamakawa K, Matsuzaki M. Influence of aortic impedance on the development of pressure-overload left ventricular hypertrophy in rats. *Circulation*. 1996;94:3362–3368.
29. Hashimoto J, Watabe D, Hatanaka R, Hanasawa T, Metoki H, Asayama K, Ohkubo T, Totsune K, Imai Y. Enhanced radial late systolic pressure augmentation in hypertensive patients with left ventricular hypertrophy. *Am J Hypertens*. 2006;19:27–32.
30. Hashimoto J, Westerhof BE, Westerhof N, Imai Y, O'Rourke MF. Different role of wave reflection magnitude and timing on left ventricular mass reduction during antihypertensive treatment. *J Hypertens*. 2008;26:1017–1024.
31. Chirinos JA, Kips JG, Jacobs DR Jr, Brumback L, Duprez DA, Kronmal R, Bluemke DA, Townsend RR, Vermeersch S, Segers P. Arterial wave reflections and incident cardiovascular events and heart failure: MESA (Multiethnic Study of Atherosclerosis). *J Am Coll Cardiol*. 2012;60:2170–2177.
32. Shah SJ, Wasserstrom JA. Increased arterial wave reflection magnitude: a novel form of stage B heart failure? *J Am Coll Cardiol*. 2012;60:2178–2181.
33. Kohno F, Kumada T, Kambayashi M, Hayashida W, Ishikawa N, Sasayama S. Change in aortic end-systolic pressure by alterations in loading sequence and its relation to left ventricular isovolumic relaxation. *Circulation*. 1996;93:2080–2087.
34. Chirinos JA, Segers P, Gillebert TC, Gupta AK, De Buyzere ML, De Bacquer D, St John-Sutton M, Rietzschel ER, Asklepios Investigators. Arterial properties as determinants of time-varying myocardial stress in humans. *Hypertension*. 2012;60:64–70.

Novelty and Significance

What Is New?

- In a middle-aged population, early systolic myocardial wall stress correlates positively, whereas late systolic wall stress correlates negatively with myocardial shortening and relaxation.
- A loading sequence characterized by a prominent late systolic load (relative to early systolic load) is associated with lower myocardial function.

What Is Relevant?

- Myocardial wall stress (what cardiomyocytes experience) during ejection cannot be derived solely from blood pressure.

- The systolic loading sequence underlies ventricular–arterial interactions in health (exercise, stress) and disease (hypertension, heart failure), and possibly underlies the development of maladaptive hypertrophy and heart failure.

Summary

The systolic loading sequence independently correlates with systolic and diastolic myocardial function.

ONLINE SUPPLEMENT

TITLE: Early and late systolic wall stress differentially relate to myocardial contraction and relaxation in middle-aged adults. The Asklepios study.

Authors: Julio A. Chirinos, MD^{*}; Patrick Segers, PhD[†]; Ernst R. Rietzschel, MD, PhD^{‡§}; Marc L. De Buyzere, PhD[‡]; Muhammad W. Raja, MD^{*}; Tom Claessens, PhD^{†,¶}; Dirk De Bacquer, PhD[§], Martin St. John Sutton, MD^{*}; Thierry C. Gillebert, MD, PhD[‡], on behalf of the Asklepios Investigators.

* Philadelphia VA Medical Center and University of Pennsylvania, Philadelphia, PA.

† Institute Biomedical Technology. Ghent University, Ghent, Belgium.

‡ Department of Cardiovascular Diseases, Ghent University Hospital, Ghent, Belgium.

§ Department of Public Health, Ghent University, Ghent, Belgium.

¶ Department of Mechanics, University College Ghent, Ghent, Belgium.

Address for correspondence:

Julio A. Chirinos, MD.
3800 Woodland Av (Rm-8B111).
Philadelphia, PA.19104.
Email: Julio.chirinos@uphs.upenn.edu;
Tel+1-215-200-7779.
Fax+215-823-4440.

Methods

Study population

We studied adults enrolled in the Asklepios study, which enrolled a population-based sample of community-dwelling adults free of clinically apparent cardiovascular disease aged 35-55 years from the Belgian communities of Erpe-Mere and Nieuwerkerken.¹ The sampling was by tiered direct mailing based on random samples drawn from the population lists. Further details about the study population have been previously published.^{1,2} All tonometry and echocardiographic measurements were performed by a single investigator (ERR). This study was approved by the ethical committee of Ghent University Hospital and the University of Pennsylvania Institutional Review Board.

Central pressure and echocardiographic measurements

Carotid artery applanation tonometry was performed using a Millar pen-type high-fidelity tonometer (SPT-301; Millar Instruments, Houston, Texas).¹ Arterial tonometry was first performed at the level of the left brachial artery, and the tonometric recording was calibrated with brachial systolic and diastolic blood pressure. Mean brachial arterial pressure was then computed by numerical integration of the brachial pressure wave form. Subsequently, carotid artery waveforms and left ventricular outflow tract pulsed wave Doppler flow velocities were simultaneously acquired. Carotid pressure wave forms were calibrated according to brachial mean and diastolic pressure.^{1,3}

Echocardiographic examinations were performed using a GE Vivid-7 ultrasound platform. Early diastolic (e') and systolic (S') septal mitral annular velocities at were measured using pulsed wave tissue Doppler from the apical 4-chamber view and were normalized for LV length.⁴ Early diastolic LV inflow propagation velocity (Vpe) was measured with color M-mode as the slope of the isovelocity line from the mitral leaflet tips to a position 4 cm distal into the LV, using the first aliasing velocity.

Although e' was our primary non-invasive measure of diastolic relaxation, we performed sensitivity analyses using Vpe. We also assessed the effect of afterload on S', which is influenced by the time-varying interaction between LV contractility and afterload during systole. Recently, S' was shown to be influenced by myocardial contractility (even in the presence of a normal ejection fraction), longitudinal fiber shortening and torsional deformation⁵ and to be an independent predictor of mortality in a general population sample with normal LV ejection fraction.⁶ In addition to S', we also assessed average longitudinal strain using speckle-tracking echocardiography as described below.

LV end-diastolic volume and LV mass were calculated with the area-length method.⁷ LV sphericity index was obtained by dividing the width of the LV measured at the basal aspect of the papillary muscles by LV length, expressed as a percentage as previously described.

Assessment of time-resolved myocardial wall stress

Speckle tracking was performed using an echoPAC workstation (GE Healthcare; Waukesha, WI) as previously described.⁸ Briefly, a region of interest was prescribed in the parasternal short-axis view at the level of the chordae tendineae to obtain an exact fit with LV wall thickness and the software was used to automatically track the wall at every time point in the cardiac cycle. Speckle tracking was also performed from the apical 4-chamber view to assess instantaneous LV

length in an interrogation angle-independent manner. Only cases in which reliable tracking of endocardial and epicardial borders was visually ascertained in both long and short axis views and in which ≤ 1 segment was labeled by the automated software as being tracked unreliably were processed further. Time-resolved numerical values derived from speckle tracking were exported from the echoPAC software for further processing in custom-designed software written in Matlab (The Mathworks, Natick, MA). We computed time-resolved short axis cross-sectional area and LV length as previously described in detail,⁸ allowing for assessments of time-resolved area-length volume measurements. The carotid pressure curve was time-aligned with geometric data using LV outflow velocity information (assessed with pulsed-wave Doppler interrogation of the outflow tract) to account for the brief delay between aortic and carotid pressure phenomena, as previously described.⁸ Time-resolved myocardial wall stress was computed according to Arts⁹:

$$\text{Myocardial Wall ("Fiber") Stress} = P / [1/3 \ln (1 + V_W/V_{LV})]$$

where P =pressure, \ln =natural logarithm, V_W =wall volume and V_{LV} =ventricular cavity volume (computed at each time point with the area-length method). This method does not neglect radially-directed forces or forces generated within the wall that oppose fiber shortening, which vary significantly with cavity and wall thickness and can interfere with direct comparisons of myocardial stress at different times during ejection.

Representative time-resolved short-axis LV wall thickness and cavity area obtained from the parasternal short-axis view are shown in figures 1A-B. Figure 1C-D show representative time-resolved changes in LV cavity size and changes in LV cavity length resulting from displacement of the base toward the apex and from apical cap thickening. Figure-2A-B shows a central pressure waveform and ejection-phase myocardial stress, respectively. To assess the myocardial loading sequence, we separately computed the myocardial stress-time integral (area under the curve) in the first half of ejection ("early" ejection-phase stress-time integral) and the 2nd half of ejection ("late" ejection-phase stress-time integral). For simplicity, throughout the remainder of the manuscript we refer to these time integrals as "early ejection-phase wall stress" and "late ejection-phase wall stress", respectively.

Speckle-tracking echocardiography data was also used to compute systolic longitudinal Langrangian strain, averaged from interrogated segments in the 4-chamber view, defined as the change of myocardial fiber length during stress in systole (L_1) compared to its original length (L_0) in a relaxed state at end-diastole¹⁰: $(L_1 - L_0)/L_0$.

Statistical analysis

The relationship between early and late systolic wall stress and indices of myocardial function was analyzed using linear regression. Multivariate models adjusted for total cholesterol, HDL-cholesterol, triglycerides, estimated glomerular filtration rate¹¹, serum C-reactive protein, current smoking, diabetes mellitus, menopausal status, antihypertensive medication use and heart rate. Although the formula we used for computation of LV myocardial stress is valid for axisymmetric ventricular geometry regardless of sphericity,⁹ we also adjusted for LV sphericity to better account for geometric factors that may impact diastolic relaxation longitudinal velocities and relaxation independently of wall stress.

In each regression model, standardized regression coefficients (β) were computed using Z scores for each of the dependent and independent variables. Standardized coefficients tell us how many standard deviations of change in the predicted variable correspond to a change of 1 standard deviation in the predictor. As opposed to "metric" regression coefficients, values of standardized regression

coefficients do not depend on the choice of units to measure each predictor and thus more intuitively compare their relative influence on the dependent variable. For all regression models presented, we assessed for important multicollinearity via computation of the variance inflation factors and tolerance values for all predictors. All variance inflation factor values were <4.2 and all tolerance values were >0.24 . All probability values are 2-tailed. Statistical significance was defined as $\alpha < 0.05$. Statistical analyses were performed using SPSS for Windows v17 (SPSS Inc., Chicago, IL).

References

1. Segers P, Rietzschel ER, De Buyzere ML, Vermeersch SJ, De Bacquer D, Van Bortel LM, De Backer G, Gillebert TC, Verdonck PR. Noninvasive (input) impedance, pulse wave velocity, and wave reflection in healthy middle-aged men and women. *Hypertension*. 2007;49:1248-1255.
2. Rietzschel ER, De Buyzere ML, Bekaert S, Segers P, De Bacquer D, Cooman L, Van Damme P, Cassiman P, Langlois M, van Oostveldt P, Verdonck P, De Backer G, Gillebert TC. Rationale, design, methods and baseline characteristics of the asklepios study. *Eur J Cardiovasc Prev Rehabil*. 2007;14:179-191.
3. Nichols WW and O'Rourke MF. *Mcdonald's blood flow in arteries. Theoretical, experimental and clinical principles*. . Oxford University Press; 2005.
4. Batterham A, Shave R, Oxborough D, Whyte G, George K. Longitudinal plane colour tissue-doppler myocardial velocities and their association with left ventricular length, volume, and mass in humans. *Eur J Echocardiogr*. 2008;9:542-546.
5. Seo JS, Kim DH, Kim WJ, Song JM, Kang DH, Song JK. Peak systolic velocity of mitral annular longitudinal movement measured by pulsed tissue doppler imaging as an index of global left ventricular contractility. *Am J Physiol Heart Circ Physiol*. 2010;298:H1608-1615.
6. Mogelvang R, Sogaard P, Pedersen SA, Olsen NT, Marott JL, Schnohr P, Goetze JP, Jensen JS. Cardiac dysfunction assessed by echocardiographic tissue doppler imaging is an independent predictor of mortality in the general population. *Circulation*. 2009;119:2679-2685.
7. Lang RM, Bierig M, Devereux RB, Flachskampf FA, Foster E, Pellikka PA, Picard MH, Roman MJ, Seward J, Shanewise JS, Solomon SD, Spencer KT, Sutton MS, Stewart WJ. Recommendations for chamber quantification: A report from the american society of echocardiography's guidelines and standards committee and the chamber quantification writing group, developed in conjunction with the european association of echocardiography, a branch of the european society of cardiology. *Journal of the American Society of Echocardiography : official publication of the American Society of Echocardiography*. 2005;18:1440-1463.
8. Chirinos JA, Segers P, Gupta AK, Swillens A, Rietzschel ER, De Buyzere ML, Kirkpatrick JN, Gillebert TC, Wang Y, Keane MG, Townsend R, Ferrari VA, Wiegers SE, St John Sutton M. Time-varying myocardial stress and systolic pressure-stress relationship: Role in myocardial-arterial coupling in hypertension. *Circulation*. 2009;119:2798-2807.
9. Arts T, Bovendeerd PH, Prinzen FW, Reneman RS. Relation between left ventricular cavity pressure and volume and systolic fiber stress and strain in the wall. *Biophys J*. 1991;59:93-102
10. Blessberger H, Binder T. Non-invasive imaging: Two dimensional speckle tracking echocardiography: Basic principles. *Heart*. 2010;96:716-722.
11. Levey AS, Coresh J, Greene T, Stevens LA, Zhang YL, Hendriksen S, Kusek JW, Van Lente F. Using standardized serum creatinine values in the modification of diet in renal disease study equation for estimating glomerular filtration rate. *Ann Intern Med*. 2006;145:247-254.

Table S1. Early and late systolic stress as predictors of early diastolic mitral annular velocity, peak systolic mitral annular velocity, peak systolic longitudinal strain and color M-mode early diastolic inflow propagation velocity in minimally adjusted models (age and gender).

Independent variables	Standardized Coefficient β	P value
Early diastolic mitral annular velocity ($R^2=0.33$)		
Late ejection-phase MWS (kdynes·cm ⁻² ·s)	-0.26	<0.0001
Early ejection-phase MWS (kdynes·cm ⁻² ·s)	0.20	<0.0001
Age (years)	-0.36	<0.0001
Male gender	-0.39	<0.0001
Peak systolic mitral annular velocity ($R^2=0.15$)		
Late ejection-phase MWS (kdynes·cm ⁻² ·s)	-0.36	<0.0001
Early ejection-phase MWS (kdynes·cm ⁻² ·s)	0.18	0.001
Age (years)	-0.06	0.017
Male gender	-0.32	<0.0001
Peak systolic longitudinal strain ($R^2=0.09$)		
Late ejection-phase MWS (kdynes·cm ⁻² ·s)	0.29	<0.0001
Early ejection-phase MWS (kdynes·cm ⁻² ·s)	-0.28	<0.0001
Age (years)	0.025	0.38
Male gender	0.25	<0.0001
Early diastolic inflow propagation velocity ($R^2=0.07$)		
Late ejection-phase MWS (kdynes·cm ⁻² ·s)	-0.12	0.04
Early ejection-phase MWS (kdynes·cm ⁻² ·s)	0.20	<0.0001
Age (years)	-0.19	<0.0001
Male gender	-0.11	<0.0001

Table S2. Early and late systolic stress as predictors of early diastolic inflow propagation velocity measured with M-mode color Doppler* (model $R^2=0.11$).

Independent variables	Standardized Coefficient	
	β	<i>P</i> value
(Constant)		
Late ejection-phase MWS (kdynes·cm-2·s)	-0.133	0.017
Early ejection-phase MWS (kdynes·cm-2·s)	0.22	<0.0001
Age (10 years)	-0.191	<0.0001
Male gender	-0.023	0.59
Body Height (m)	-0.104	0.025
Body weight (10 kg)	0.017	0.718
Total cholesterol (10 mg/dl)	-0.054	0.083
HDL-cholesterol (10mg/dl)	0.102	0.004
Triglycerides (10 mg/dl)	0.052	0.11
Estimated GFR, mL·min⁻¹·1.73 m⁻²	0.022	0.43
High-sensitive CRP (ln-transformed; mg/dl)	0.04	0.18
Current smoking	0.038	0.19
Diabetes mellitus	0.035	0.21
LV sphericity (10%)	-0.141	<0.0001
Antihypertensive medication use	0.039	0.17
Heart rate (10 bpm)	-0.07	0.019

* Analysis based on 1,196 subjects with available color M-mode data and time-resolved wall stress data.